Available online at www.sciencedirect.com

ScienceDirect

Energy Procedia 38 (2013) 216 – 222

Energy Procedia

SiliconPV: March 25-27, 2013, Hamelin, Germany

Numerical simulation of vertical silicon nanowires based heterojunction solar cells

Mauro Zanuccoli[a,*], Jérôme Michallon[b], Igor Semenihin[c], Claudio Fiegna[a], Anne Kaminski-Cachopo[b], Enrico Sangiorgi[a], Vladimir Vyurkov[c]

[a] *Advanced Research Center on Electronic Systems – Department of Electrical, Electronic, and Information Engineering "Guglielmo Marconi", University of Bologna, 47512 Cesena (FC), Italy*
[b] *Institut de Microélectronique Electromagnétisme et Photonique - Laboratoire d'Hyperfréquences et de Caractérisation, Grenoble INP Minatec, 3 parvis Louis Néel, BP 257, 38016 Grenoble, France*
[c3] *Institute of Physics and Technology Russian Academy of Sciences, Moscow 117218, Russia*

Abstract

Nanowires (NWs) solar cells are expected to outperform the thin-film counterparts in terms of optical absorptance. In this theoretical study we optimize the geometry of vertical crystalline-amorphous silicon core-shell NW arrays on doped ZnO:Al (AZO)-Glass substrate by means of 3-D optical simulations in order to maximize the photon absorption. The optimized geometry is investigated by means of 3-D TCAD numerical simulation in order to calculate the ultimate efficiency and the main figures of merit by taking into account recombination losses. We show that optimized 10 μm-long crystalline – amorphous silicon core-shell (c-Si/a-Si/AZO/Glass) NWs can reach photo-generated current up to 22.94 mA/cm^2 (above 45% larger than that of the planar counterpart with the same amount of absorbing material) and conversion efficiency of 13.95%.

Keywords: Silicon Nanowires; 3-D Electro-Optical Simulation; heterojunction core-shell nanowire.

1. Introduction

Silicon nanowire (NW) arrays may be promising low-cost alternatives to wafer-based solar cells [1], indeed sparse arrays of NWs allow to reach relatively high conversion efficiency with smaller amount of

* Corresponding author. Tel.: +39-0547-339539; fax: +39-0547-339533 .
E-mail address: mazanuccoli@arces.unibo.it .

doi:10.1016/j.egypro.2013.07.270

absorbing material. The geometrical features of NW arrays allow the incident light to be coupled into Bloch modes [2] and thus to enhance the absorption. Optimization of NW arrays involves the proper sizing of the geometrical parameters such as periodicity and diameter. As the dimensions of the investigated structures are comparable with the radiation wavelength λ, optical simulations must be performed by rigorously solving the Maxwell equations using for example FDTD method [3] or RCWA [4]. The second method is based on the modal expansion of the electromagnetic field into spatial harmonics. In the case of RCWA the approximation is introduced by the number of Fourier modes considered in the calculation enabling to attain a good trade-off between accuracy and computational resources. RCWA has been used in [5] to simulate InP NWs. In [6] a-Si NW arrays have been theoretically investigated by means of 2-D optical and TCAD simulators. In [7] a theoretical analysis of the light trapping in GaAs NW arrays has been performed by 3-D FDTD simulations followed by electric simulations with a commercial device simulator. Kelzenberg and coauthors in [8] have used 3-D FDTD simulations in order to calculate the generation rate map of silicon NWs and have incorporated the spatially resolved optical generation map in a TCAD tool by exploiting the cylindrical symmetry of the wire.

In this work we optimize a 10 μm-long c-Si/a-Si/AZO/Glass NWs array by means of 3-D electro-optical simulations. Differently from [7-8], optical simulations have been performed by RCWA rather than by using the CPU-intensive FDTD method. An extensive analysis of different geometries has been carried out without limiting the investigation to a restricted set of NW diameters as in [6]. The optimized geometry has been investigated by means of Sentaurus Device [9] in order to predict the main figures of merit by accounting for state-of-the-art physical models.

2. Simulated device and simulation methodology

The simulated device (Fig. 1) is an array of cylindrical NWs on AZO/Glass substrate with periodicity *P* (along both *x, y* directions) and radial junction. The core is p-type doped crystalline silicon (c-Si) while the amorphous silicon (a-Si) shell includes a 8 nm-thick n-type doped layer and a 32 nm-thick intrinsic interfacial layer (i-layer). The conformal 200 nm-thick Al-doped ZnO layer is used as transparent front electrode. *P* is varied from 200 nm to 700 nm and the ratio of the shell diameter (D_{shell}) to *P* from 0.4 up to 1.0. Shell and core are uniformly doped (doping concentration N_s=3x10^{19} cm^{-3} and N_c=10^{16} cm^{-3}, respectively).

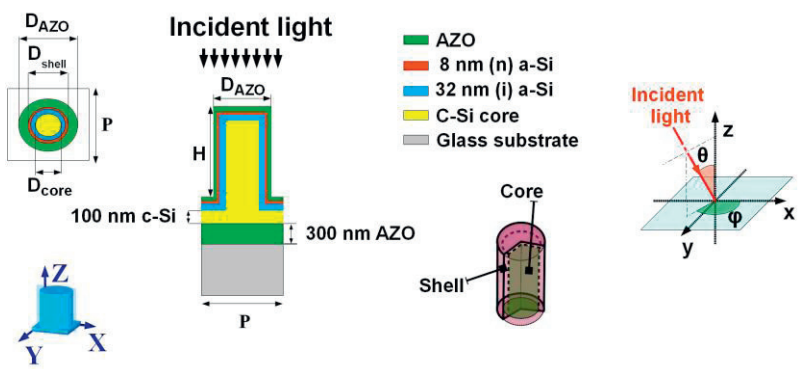

Fig. 1. Sketch of the simulated NWs. The amorphous silicon (a-Si) shell includes a 8 nm-thick n-doped layer (n) and a 32 nm-thick intrinsic layer (i). The angle of incidence of light with respect to the normal to device plane is denoted by θ.

2.1. Optical simulation setup

Optical simulations have been performed by means of an in house developed RCWA simulator validated by means of comparison with literature and FDTD calculations [10]. In order to reduce the computational effort we adopt $N=N_x \times N_y=15\times15$ Fourier modes for $\lambda < 700$ nm and $N=N_x \times N_y=41\times41$ above, where a larger number of modes is required to reach an acceptable accuracy. In addition RCWA exploits the *x* and *y* mirror symmetries of the structure illuminated normally to the device plane. We adopt direct illumination, standard ASTM G173-03 spectrum with irradiance $1000 W/m^2$. Calculations of absorptance and of photogenerated current density have been carried out by assuming a wavelength span from 300 nm to 1100 nm with interval of 10 nm, ensuring an adequate accuracy even above 700 nm where rapid fluctuations of the absorptance can be averaged over the wavelength. In order to calculate the absorptance, only electron-hole pairs generated within the silicon are accounted for. The cut-off wavelength for the photon absorption in a-Si is 725 nm while it is of 1100 nm for c-Si. For c-Si we adopt the optical database from Palik [11]. The calculated 3-D optical generation rate is flattened to 2-D cylindrical coordinates using a spatial integration procedure which permits the conservation of the total photo-generated carriers throughout the volume of the NW [8].

2.2. Electrical simulation setup

Electrical simulations have been performed assuming the cylindrical symmetry of the structure. Simulations account for Auger recombination, single-level trapping Shockley-Read-Hall (SRH) recombination in c-Si, surface recombination at AZO/silicon interfaces, thermionic emission and heterojunction specifications at a-Si/c-Si interface. Fermi-Dirac statistics is adopted. In the p-doped c-Si region the minority carrier lifetime (SRH recombination) is set to 10 μs while in a-Si a continuous distribution of density of states (DOS) is adopted by assuming exponential band-tails (BT) and Gaussian mid-gap (MG) dangling-bonds (DB) states. The maximal concentration of Gaussian traps in the n-doped a-Si shell is 10^{18} $cm^{-3}eV^{-1}$ and 10^{17} $cm^{-3}eV^{-1}$ for donor-like and acceptor-like states, respectively, while in the i-layer it is assumed at least an order of magnitude smaller [12]. In all a-Si regions, the concentration of band-tail defects is 10^{21} $cm^{-3}eV^{-1}$. Carrier mobility is 10 (1) $cm^2V^{-1}s^{-1}$ in n-type doped a-Si and 20 (2) $cm^2V^{-1}s^{-1}$ in i-layer for electrons (holes) (Tab. 1). In c-Si the doping-dependent mobility model proposed by Klassen [13] has been adopted. The calculated mobility for carriers in c-Si is reported in Tab. 1. The electron affinity and the energy band gap for a-Si are 3.85 eV and 1.72 eV, respectively. In a-Si, the effective density of states in the conduction and valence bands (at T=300 K) is $2x10^{20}$ cm^{-3}. In order to perform the device simulation, AZO layers have been replaced by electrodes treated as ideal ohmic contacts. In this study, contact resistivity has been neglected.

Table 1. Physical parameters in silicon and surfaces recombination velocities adopted at interfaces for minority carriers.

Parameter	Symbol	Unit	Ideal NW			Baseline		
			n-doped a-Si	i-layer a-Si	c-Si	n-doped a-Si	i-layer a-Si	c-Si
Holes band mobility	μ_p	$cm^2V^{-1}s^{-1}$	100	100	385	1	10	385
Electron band mobility	μ_n	$cm^2V^{-1}s^{-1}$	100	100	1261	2	20	1261
Front SRV (a-Si/AZO) for holes	$FSRV_p$	cm/s		10^1			10^7	
Back SRV (c-Si/AZO) for electrons	$BSRV_n$	cm/s		10^1			10^3	

In the following, the baseline configuration denotes the device for which the values of the physical parameters have been adopted as described in literature [12]. The ideal NW configuration refers to the configuration where a-Si traps are neglected and with the carrier mobility of 100 $cm^2V^{-1}s^{-1}$, for both holes and electrons (Tab. 1). The surface recombination velocities (SRVs) are set as shown in Tab. 1 (SRVs for majority carriers are set to 10^7 cm/s everywhere). For both ideal and baseline NWs, the interface between the a-Si and the c-Si is assumed to be lossless.

3. Discussion and results

The calculated photo-generated current densities within the considered geometrical parameters range are shown in Fig. 2a. A plateau of the photo-generated current density around the optimum geometry (P=450 nm and D_{shell}/P =0.8, leading to Jph=22.94 mA/cm^2) can be observed. As shown in Fig. 2b, the absorptance calculated for an optimized NW array is higher (approximately 45%) than that obtained by the planar counterpart. In addition, a peak of absorptance (0.97) at approximately 540 nm can be observed. Absorptance has been computed by considering only the electron-hole pairs generated in the silicon (shell and core). It is worth noting that the calculated absorptance is markedly above 0.4 within the spectral range 450 nm – 800 nm; however, due to the relatively high imaginary part of the a-Si complex refractive index, most of the solar optical power is absorbed by the NW shell in particular up to the cut-off wavelength of the a-Si (730 nm). For radiation wavelength above 730 nm the absorption occurs mainly in the c-Si core region. Since in c-Si the absorption depth is larger than 10 μm, the remaining radiation is not absorbed and can be transmitted through the silicon/AZO interface at the bottom or reflected back to the NW due to Fresnel reflection. Therefore, oscillations in the absorptance characteristics are probably ascribed to Fabry-Perrot resonances that enhances the optical path. The calculated reflectance (R) and transmittance (T) are shown in Fig. 2c.

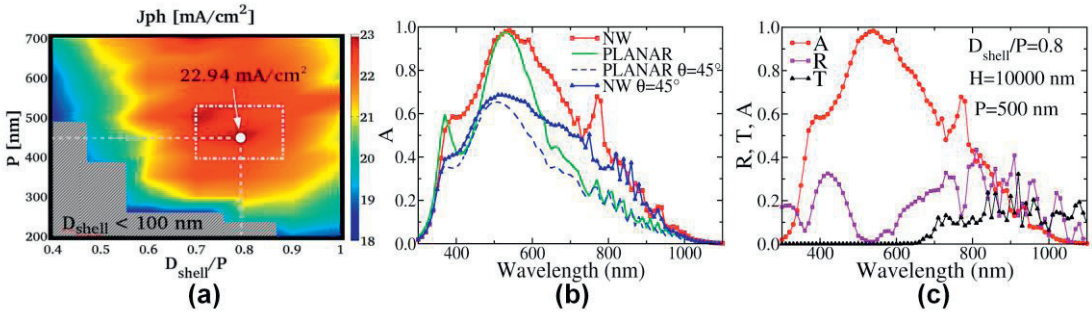

Fig. 2. (a) Map of the calculated photo-generated current density Jph versus the periodicity P and the ratio of shell diameter (D_{shell}) to P. The NWs height H is 10 μm. (b) Optical absorptance A for the NW array (P=500 nm, H=10 μm, D_{shell}/P=0.8) under normal illumination and with angle of incidence of the radiation θ=45 degree (Fig. 1). The comparison with planar counterpart is shown. (c) Reflectance R, transmittance T and absorptance A of the NW array.

For the electrical simulation the structure featuring P=500 nm and D_{shell}/P =0.8 (close to the optimum one) has been considered. The corresponding photo-generated current density Jph is 22.62 mA/cm^2. Tab. 2 reports the figures of merit of the ideal NW for which the bulk recombination losses are neglected. The calculated efficiency for the ideal NW configuration is 13.95%, while the baseline configuration results in a conversion efficiency of 9.83%. The lower efficiency of the baseline NW is ascribed to the recombination losses at interfaces (a-Si/AZO, c-Si/AZO), to the carrier recombination due to defects in a-Si as well as to a significantly lower carriers mobility in a-Si with respect to the ideal case. In order to

investigate the influence of defects at interfaces on main figures of merit, the front surface recombination velocity (FSRV) at the interface between n-doped a-Si and AZO has been set to either 10 cm/s or 10^7 cm/s while the back surface recombination velocity (BSRV) at interface between c-Si layer and bottom AZO layer has been considered as either 10 cm/s or 10^6 cm/s. The remaining physical parameters are those of the baseline NW used as reference configuration in the following discussion. We observe that the impact of the BSRV on performance is remarkable (Fig. 3a). In particular, Voc drops from approximately 700 mV down to 400 mV with increasing BSRV, leading to a conversion efficiency (η_c) ranging from 6.58 % to 11.12 %. The impact of the FSRV on performance is mitigated by the shell passivation effectiveness (values of photo-generated current density and efficiency are around 19.9 mA/cm^2 and 9.90 %, respectively, as shown on Fig. 3b). Regardless the value of the FSRV, Voc is equal to 602 mV as for baseline. One drawback of amorphous materials is the presence of high defect concentration, especially in doped regions such as the n-doped shell. While the traps in the intrinsic buffer layer (i-layer) do not play a crucial role in determining the performance, the defect distribution in the doped region may potentially results in an efficiency degradation. The impact of the dangling bonds concentration on short-circuit current density in the doped a-Si shell (N_{DB}) is highlighted by the carrier collection efficiency η_c (defined as the ratio of the collected carriers at electrodes to the amount of those photogenerated in the silicon). If N_{DB} increases of three orders of magnitude, from 10^{17} (10^{18}) cm^{-3}eV^{-1} to 10^{20} (10^{21}) cm^{-3}eV^{-1} for acceptor-like (donor-like) states, η_c decreases significantly at short wavelength values (below 700 nm) since the trap assisted electron-hole pairs annihilation becomes relatively large in the region of the NW where the absorption mainly occurs for high energy photon. If N_{DB} is of 10^{20} (10^{21}) cm^{-3}eV^{-1} for acceptor-like (donor-like) states, the calculated efficiency decreases from 9.83 % to 7.54 % (Tab. 2).

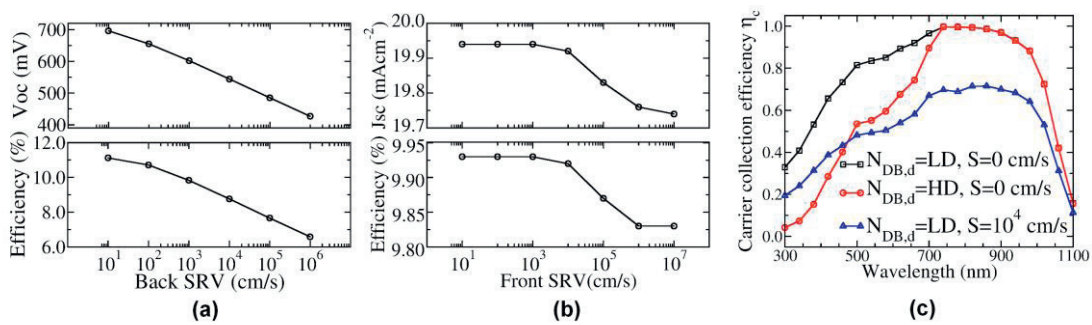

Fig. 3. Influence (a) of the BSRV at the c-Si/AZO interface and (b) of the front FSRV at the shell/AZO top interface on main figures of merit. Simulations have been performed by adopting the physical parameters of the baseline NW. (c) Carrier collection efficiency for the c-Si/a-Si NW (P=500 nm, D_{shell}/P =0.8) calculated for the baseline NW configuration. S denotes the surface recombination velocity at the interface between the intrinsic a-Si layer and the c-Si core, while $N_{DB,d}$ denotes the Gaussian maximum density of the dangling bonds donor-like states per unit of volume and energy in the n-doped a-Si layer (LD=10^{18} cm^{-3} eV^{-1}, HD=10^{21} cm^{-3}eV^{-1}); the maximum density of the dangling bonds acceptor-like states is assumed to be one order of magnitude lower than $N_{DB,d}$.

Finally, the potentially high defective interface between the i-layer and c-Si (that has been assumed lossless in ideal and baseline NWs) may lead to a significant degradation of Jsc. In addition, it is worth noting that the SRV at the interface between the i-layer and the c-Si core (denoted by SRV(a-Si/c-Si)) (Fig. 1) is an effective loss mechanism within the entire spectrum as confirmed by the characteristics in Fig. 3c, in which the collection efficiency calculated for SRV(a-Si/c-Si)=0 cm/s (ideal interface) is compared to that for 10^4 cm/s (relatively high-defective interface). In the second case, Jsc and Voc drop to 12.60 mA/cm^2 and to 528 mV, respectively, while the efficiency is reduced to 5.35 % (Tab. 2).

Table 2. Main figures of merit of the NW array (P=500 nm, D_{shell}/P=0.8) calculated by simulator .

NW	J_{sc} (mA/cm^2)	V_{oc} (mV)	FF (%)	η (%)
Ideal	22.62	725	85.1	13.95
Baseline	19.74	602	82.7	9.83
Baseline with $N_{DB,d}=10^{21}$ cm^{-3}eV^{-1}	15.61	594	81.2	7.54
Baseline with SRV(a-Si/c-Si)=10^4 cm/s	12.60	528	80.4	5.35

4. Conclusions

In this theoretical study, c-Si/a-Si core-shell vertical NW arrays based solar cells on AZO/Glass substrate have been optimized by means of 3-D RCWA optical simulations. The NW arrays analyzed in this work exhibit significant photon absorption improvement compared with the planar counterparts. Electrical simulations of an optimized NW with radial junction have been carried out in order to highlight the influence of the recombination losses at potentially high-defective interfaces as well as that of the trap density in the doped a-Si shell on the main figures of merit. Numerical simulations have shown that conversion efficiency is not markedly affected by surface recombination velocities at the interface between a-Si and AZO. The calculated efficiency for the ideal setup of the 10 μm-long nanowire arrays studied in this work is 13.95%.

Acknowledgements

Support from NANOFUNCTION FP7-NOE is gratefully acknowledged.

References

[1] Erik C. Garnett, M. L. Brongersma, Y. Cui and M. D. McGeheee, Nanowire Solar Cells, *Annual Review of Material Research*, 41:11.1–11.27, 2011.

[2] B. C. P. Sturmberg, K. B. Dossou, L. C. Botten, A. A. Asatryan, C. G. Poulton, C. M. de Sterke, R. C. McPhedran, Modal analysis of enhanced absorption in silicon nanowire arrays, *Optics Express* 19, A1067-1081, 2011.

[3] K. S. Kunz and R. J. Luebbers. *The Finite Difference Time Domain Method for Electromagnetics*. CRC Press, 1993.

[4] M. G. Moharam and T. K. Gaylord, Rigorous coupled-wave analysis of planar-grating diffraction, *J. Opt. Soc. Am.*, 71 (7), pp. 811-818, 1981.

[5] P. Kailuweit, M. Peters, J. Leene, K. Mergenthaler, F. Dimroth and A. W. Bett, Numerical simulations of absorption properties of InP nanowires for solar cell applications, *Prog. Photovolt: Res. Appl*. doi: 10.1002/pip.1169, 2011.

[6] Z. Pei, S.-T Chang, C.-W Liu and Y.-C Chen, Numerical simulation on the photovoltaic behavior of an amorphous-silicon nanowire-array solar cell, *IEEE Electron Device Letters*, vol. 30, 12, pp.1305-1307, 2009.

[7] L. Wen, Z. Zhao, X. Li, Y. Shen, H. Guo and Y. Wang,Theoretical analysis and modeling of light trapping in high efficiency GaAs nanowire array solar cells, *Appl. Phys. Lett*. 99, 143116, 2011.

[8] M. D. Kelzenberg, M. C. Putnam, D. B. Turner-Evans, N. S. Lewis and H. A. Atwater, Predicted efficiency of Si ire array solar cells, *Proc. of 34th IEEE Photovoltaic Specialists Conference (PVSC)*, pp. 1948-1953, 2009.

[9] Sentaurus Device User Guide, Version C-2009.06. Synopsys. Inc., 2009.

[10] J. Michallon, M. Zanuccoli, A. Kaminski-Cachopo, V. Consonni, A. Morand, D. Bucci, F. Emieux, H. Szambolics, S. Perraud and I. Semenikhin, Comparison of optical properties of Si and ZnO/CdTe core/shell nanowire arrays, *Mater. Sci. Eng. B* (2012), http://dx.doi.org/10.1016/j.mseb.2012.10.037 (in press).

[11] E. D. Palik, *Handbook of Optical Constants of Solids*, Elsevier, 1988.

[12] A. Fantoni, M. Vieira and R. Martins, Simulation of hydrogenated amorphous and microcrystalline silicon optoelectronic devices, *Mathematics and Computer Simulations* 49, 381.401, 1999.

[13] D. B. M. Klassen, A unified mobility model for device simulation: I. model equations and concentration dependence. *Solid-State Elec*. 35 (7), 1992, pp. 953-959.